

Crack closure in fibre metal laminates

H.M. PLOKKER, R.C. ALDERLIESTEN and R. BENEDICTUS

Structures and Materials Laboratory, Faculty of Aerospace Engineering, Delft University of Technology, P.O. Box 5058, 2600 GB Delft, The Netherlands

Received in final form 28 March 2007

ABSTRACT GLARE is a fibre metal laminate (FML) built up of alternating layers of S2-glass/FM94 prepreg and aluminium 2024-T3. The excellent fatigue behaviour of GLARE can be described with a recently published analytical prediction model.

This model is based on linear elastic fracture mechanics and the assumption that a similar stress state in the aluminium layers of GLARE and monolithic aluminium result in the same crack growth behaviour. It therefore describes the crack growth with an effective stress intensity factor (SIF) range at the crack tip in the aluminium layers, including the effect of internal residual stress as result of curing and the stiffness differences between the individual layers. In that model, an empirical relation is used to calculate the effective SIF range, which had been determined without sufficiently investigating the effect of crack closure.

This paper presents the research performed on crack closure in GLARE. It is assumed that crack closure in FMLs is determined by the actual stress cycles in the metal layers and that it can be described with the available relations for monolithic aluminium published in the literature.

Fatigue crack growth experiments have been performed on GLARE specimens in which crack growth rates and crack opening stresses have been recorded. The prediction model incorporating the crack closure relation for aluminium 2024-T3 obtained from the literature has been validated with the test results.

It is concluded that crack growth in GLARE can be correlated with the effective SIF range at the crack tip in the aluminium layers, if it is determined with the crack closure relation for aluminium 2024-T3 based on actual stresses in the aluminium layers.

Keywords crack closure; crack growth; fatigue; fibre metal laminates; glare; stress ratio.

- NOMENCLATURE**
- a = half crack length (mm)
 - C_{cg} = Paris constant in crack growth relation
 - C_d = Paris constant in delamination growth relation
 - E = Young's modulus (MPa)
 - G_d = maximum energy release rate for delamination (MPa mm)
 - K = stress intensity factor (MPa mm)
 - n = number of layers
 - n_{cg} = Paris constant in crack growth relation
 - n_d = Paris constant in delamination growth relation
 - R = stress ratio (S_{min}/S_{max})
 - S = stress (also σ) (MPa)
 - t = thickness (mm)
 - U = ratio between effective stress range and total stress range

- v_0 = reference potential drop (mV)
 v_a = potential drop over crack (mV)
 da/dN = crack growth rate ($\mu\text{m}/\text{cycles}$)
 db/dN = delamination growth rate ($\mu\text{m}/\text{cycles}$)
 β = Geometry correction factor
 $v(x_i, y_i)$ = displacement at location x_i, y_i (mm)

INTRODUCTION

Since the eighties of the last century, the fibre metal laminate (FML) concept has been under constant development at Delft University of Technology. This development surged in 1996 with studies for the application of GLARE on the Airbus A380 (Airbus Headquarters, Blagnac Cedex, France).¹ The material GLARE is an FML built up of thin sheets of aluminium 2024-T3 (thickness range 0.3–0.5 mm) and S2-glass fibre layers pre-impregnated with FM94 epoxy (prepreg). Due to its good static strength and damage tolerance characteristics, GLARE is used as upper fuselage skin material in the A380. Other favourable advantages compared to monolithic aluminium are the excellent resistance against fire, impact, lightning and corrosion. The latter is the result of the layered composition of the material: it contains natural barriers in thickness direction.²

In GLARE, the fatigue crack propagation phase covers the major part of the fatigue life, which is opposite to monolithic aluminium where fatigue initiation is most important.³ Fatigue damage in GLARE is characterized by the crack growth in the aluminium layers and delamination growth between the aluminium and prepreg layers. A crack in the aluminium layers is 'bridged' by the fibres, which carry a significant amount of the load (see Fig. 1). Crack growth in GLARE is a self-balanced mechanism between crack growth in the metal layers and the delamination growth at the interfaces. The result is an

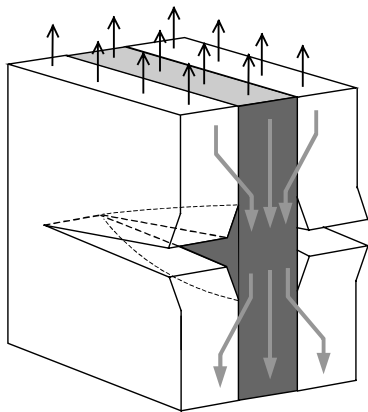


Fig. 1 Illustration of fibre bridging of a crack in a GLARE laminate.

approximately constant stress intensity factor (SIF) and crack growth rate for long ranges of crack lengths.

The fatigue properties of GLARE can be described with a similarity approach: similar stress states in the aluminium layers of a GLARE laminate and in monolithic material will lead to the same crack growth rates. For crack growth under constant amplitude (CA) loading, Alderliesten^{4,5} presented a theoretical model to determine the SIF at the crack tip. With the SIF range, the crack growth can be determined with material constants C and n , in the linear Paris- ΔK region.⁶

The concept of crack closure, which has been introduced by Elber⁷ for monolithic aluminium, describes the effect of plasticity at the crack tip acting in the wake of the crack as it propagates. As a result of crack closure, the crack opening stress is above the minimum stress, which means that the stress range that contributes to crack growth is reduced. The effective SIF range ΔK_{eff} is related to the effective stress range and incorporates the effect of the stress ratio.

At the moment, the analytical prediction model for GLARE can only be used for prediction of crack growth under CA loading and uses an empirical relation to determine the effective stress range.⁸ The effect of crack closure is assumed to be covered by this empirical relation, but had not yet been investigated for GLARE. To support development of a theoretical variable amplitude (VA) model for GLARE, it has been decided to investigate crack closure first.

The research on crack closure in GLARE, presented in this paper, is based on the similarity approach, assuming that for equal stress state the crack closure behaviour in the aluminium layers of GLARE is similar to monolithic aluminium.

CRACK CLOSURE

Prediction of crack growth

Crack propagation in metals is described with the SIF introduced by Irwin.⁶ Crack growth experiments revealed that different stress ratios result in different crack growth rates, which means that the crack growth rate is a function of ΔK and for the stress ratio. Between the threshold phase of the material and the fracture toughness phase, the crack growth rate can be described with the linear Paris- ΔK

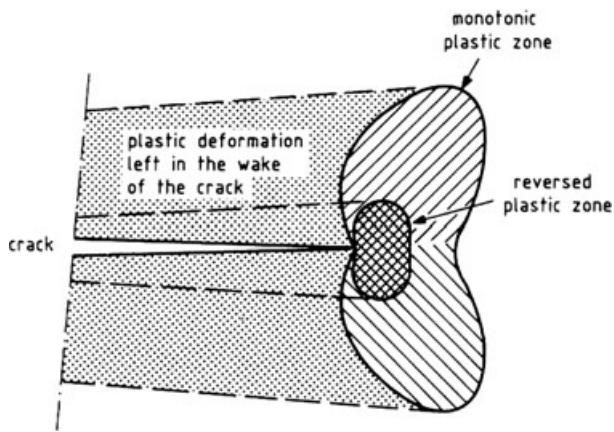


Fig. 2 Illustration of reversed and monotonic plastic zone.⁷

relation. The Paris relation has the limitation that it does not account for the stress ratio effect on crack growth. This means that each stress ratio has a different da/dN - ΔK curve.

Elber stated that crack extension can only take place in that portion of the load cycle in which the crack is fully open, which he called the effective stress range.

$$\Delta S_{\text{eff}} = S_{\text{max}} - S_{\text{op}} \quad \text{for } S_{\text{op}} \geq S_{\text{min}}. \quad (1)$$

Two zones can be distinguished in the plastic zone at the crack tip (see Fig. 2). The first zone is the monotonic plastic zone that is formed at the crack tip as the result of a load. After unloading, high compressive residual stresses around the plastic deformed material can form a reversed plastic zone. Elber estimated the reversed plastic zone about one quarter of the monotonic plastic zone. As the crack propagates, monotonic and reversed plastic deformed material is left in the wake of the crack that presses together the crack flanks at stress levels below the crack opening stress.

The plastic zone created at the crack tip is dependent on the stress intensity and therefore increases with the crack length for CA fatigue loading. The reversed crack tip plasticity depends on the minimum applied stress and as a consequence the plastic wake field is dependent on the stress ratio. Therefore, the effective stress range includes stress ratio effects. This means that the crack growth behaviour of a metal can be described by a single da/dN - ΔK_{eff} curve.

Elber⁷ called the ratio between the effective stress range and the total stress range, the effective stress range ratio. After experiments on aluminium 2024-T3, Newman⁹ and later Schijve¹⁰ proposed the following relation:

$$U = \frac{\Delta S_{\text{eff}}}{\Delta S} = \frac{(S_{\text{max}} - S_{\text{op}})}{(S_{\text{max}} - S_{\text{min}})} = 0.55 + 0.33R + 0.12R^2. \quad (2)$$

The effective stress range is in general dependent on the stress ratio.^{11,12} Schijve¹³ remarked that the opening stress

S_{op} is not a function of the stress ratio for high values of K_{max} .

The SIF only contributes to crack growth when the crack is open. As a consequence, the crack driving force is ΔK_{eff} and the Paris relation becomes:

$$\begin{aligned} \frac{da}{dN} &= C (\Delta K_{\text{eff}})^n = C (U \Delta K)^n \\ &= C [(0.55 + 0.33R + 0.12R^2) \Delta K]^n. \end{aligned} \quad (3)$$

Crack closure in the literature

Despite other literature,¹⁴ the experiments of Trebules *et al.*,¹⁵ Arkema and Schijve,¹⁶ Gan and Weertman¹⁷ have confirmed the role of crack closure as interaction effect. A remarkable experiment was presented by Blazewicz¹⁸ with ball impressions on aluminium 2024-T3. He reported only a small delay during the growth through the overload plastic zone, while a significant delay occurred at a later stage. This could indicate that crack closure is active in the wake of the crack, and the residual stresses ahead of the crack tip have relatively little significance.

Plasticity-induced crack closure is the only mechanism that can explain the so called 'delayed retardation', after an overload. It happens that the cracks grow an initial distance, sometimes at higher rate, before the deceleration of the crack growth rate takes place. This effect is attributed to the plastic zones, which are created at the tip in the overload cycle and which have a crack closing effect in the wake of the crack.

Other crack closure mechanisms besides plasticity-induced crack closure are roughness-induced crack closure and crack filling closure. Roughness-induced closure is the result of a mismatch of the fracture surface asperities at unloading, and is related to low stress intensity ranges close to the threshold SIF ΔK_{th} .¹²

Crack filling closure is induced by external agents that produce corrosion products, oxides and fretting debris. By filling the crack, the effective stress intensity range is reduced. This closure phenomenon is only relevant for corrosion sensitive materials in a wet environment.¹⁹⁻²¹ As the order of magnitude of both mechanisms is believed to be insignificant for the current work, this will not be discussed further.

Crack opening in GLARE

Especially for thick plates, the crack opening is a three-dimensional phenomenon. The plastic zone at the crack tip is dependent on the stress conditions in the metal, which varies through the thickness.

It is assumed that in thin sheets the crack opening is related to plane stress behaviour only. In addition, the outer layers are less restrained than the inner layers, because they are supported by fibre layers at one side only. This

means that the crack opening takes place at a lower stress level and consequently the crack length is larger compared to the inner layers. Therefore, it is conservative to assume, that the crack opening in the outer layers of a GLARE laminate are representative for the crack opening in the internal aluminium layers.

GLARE

The material GLARE is one variant of the FML concept and is manufactured of alternating aluminium 2024-T3 layers and a prepreg of S2-glass fibres with FM94 epoxy adhesive. GLARE is cured in an autoclave at 120 °C and 6 bar.²

The glass fibre layers in the laminate can be positioned in different orientations. A system has been defined to give order to the different combinations and orientations of aluminium and fibre layers. The system is based on a notation with four variables: GLARE X-X/X-X. The outer layers of a GLARE laminate are always made of aluminium to prevent moisture intrusion in the prepreg.

The first variable defines the GLARE type, which determines the fibre orientation between two aluminium layers (Table 1). The fibre orientation is defined with respect to the rolling direction of the aluminium layers and each orientation represents a prepreg layer with a nominal thickness of 0.133 mm. The second and third variable characterizes respectively the number of aluminium and prepreg layers. The last variable gives the thickness of the aluminium layers in the laminate.

In FMLs, the actual stresses in the metal layers are different from the applied laminate stresses, as result of differences in stiffness and thermal expansion coefficients of the constituents. The stress cycle in aluminium layers as a result of the applied stress cycle on the laminate can be calculated with the classical laminate theory. The curing of the laminate causes a tensile stress in the aluminium layers. The stress cycle in the aluminium layer is calculated with superposition of curing stress and stress due to stiffness differences.

ANALYTICAL PREDICTION MODEL

With the recently published analytical model,^{4,5} the crack growth in GLARE can be predicted for CA loading. The analytical model successively describes the bridging stress, the delamination shape extension, the SIF and the crack growth. From this work, it was concluded that the bridging stress, the crack opening contour, and the delamination shape are in balance with each other.

The bridging stress is obtained by equalling the relations for the crack opening in the metal layers and the elongation and deformation of the fibre layers. Rewriting results in a solution for the bridging stresses, which is not a closed form. To solve this problem numerically, the crack is divided in *N* bar elements, over which the crack opening is calculated and summated.

The fibre layers in an FML transfer most of the load through the crack in the metal layers. Therefore, the fibre bridging stress has a direct influence on the SIF at the crack tip. However, the bridging stress is influenced by the shape of the delamination, which therefore has a significant influence on the crack growth.

To determine the delamination growth, the energy release rate, *G*, has been used.²² The tensile residual curing stresses in the aluminium layers cause bridging stresses greater than zero, although the laminate stress is equal to zero. Therefore the maximum and minimum energy release rate is determined including this bridging stress.

$$G_{\max}(x) = \frac{n_f t_f}{2j E_f} \left(\frac{n_{al} t_{al} E_{al}}{n_{al} t_{al} E_{al} + n_f t_f E_f} \right) (S_f + S_{br,\max}(x))^2 \tag{4}$$

$$G_{\min}(x) = \frac{n_f t_f}{2j E_f} \left(\frac{n_{al} t_{al} E_{al}}{n_{al} t_{al} E_{al} + n_f t_f E_f} \right) (RS_f + S_{br,\min}(x))^2. \tag{5}$$

The delamination growth is then described with a Paris type relation:

$$\frac{db}{dN}(x) = C_d (\sqrt{G_{d,\max}(x)} - \sqrt{G_{d,\min}(x)})^{n_d}, \tag{6}$$

Table 1 Different GLARE types, sheet thicknesses, fibre orientations, and specific characteristics²

| GLARE grade | Metal sheet thickness variation | Prepreg orientation in each fibre layer | Characteristics |
|----------------------|---------------------------------|---|----------------------------|
| GLARE 2A | 0.2–0.5 | 0°/0° | Fatigue, strength |
| GLARE 2B | 0.2–0.5 | 90°/90° | Fatigue, strength |
| GLARE 3 ¹ | 0.2–0.5 | 90°/0° | Fatigue, impact |
| GLARE 4A | 0.2–0.5 | 0°/90°/0° | Fatigue, strength in L-T |
| GLARE 4B | 0.2–0.5 | 90°/0°/90° | Fatigue, strength in T-L |
| GLARE 5 | 0.2–0.5 | 0°/90°/90°/0° | Impact |
| GLARE 6A | 0.2–0.5 | +45°/-45° | Shear, off-axis properties |
| GLARE 6B | 0.2–0.5 | -45°/+45° | Shear, off-axis properties |

¹In GLARE 3 laminates, the fibre layer closest to the outer aluminium layer of the laminate is in the rolling direction of the aluminium.

where the constants C_d and n_d have been determined with experiments²² and are determined at room temperature to be respectively 0.05 and 7.5 for GLARE.

According to the theoretical model, the effective SIF in GLARE is defined as the difference between the far-field SIF and the bridging SIF.

$$K_{\text{tip}} = K_{\text{farfield}} - K_{\text{bridging}}, \quad (7)$$

where for an infinite plate:

$$K_{\text{farfield}} = S_{\text{al}} \sqrt{\pi a} \quad (8)$$

and:

$$K_{\text{bridging}} = 2 \sum_{i=1}^N \frac{S_{\text{br,al}}(x_i)w}{\sqrt{\pi a}} \frac{a}{\sqrt{a^2 - x_i^2 + b_i^2}} \left(1 + \frac{1}{2} (1 + \nu) \frac{b_i^2}{a^2 - x_i^2 + b_i^2} \right), \quad (9)$$

where $S_{\text{br,al}}$ is the bridging stress defined as the amount of stress transferred from the aluminium layers to the fibre layers, a the half crack length, and b the delamination width.

The SIFs are corrected for the finite width of the specimen by a correction factor β .²³ From the stress intensity at the crack tip, the effective stress intensity is calculated with the empirical relation of De Koning.⁸

$$\Delta K_{\text{eff}} = (1 - R^{1.35}) K_{\text{tip}}. \quad (10)$$

With the effective stress intensity range, the crack growth rate can be determined with the material constants C_{cg} and n_{cg} for the Paris- ΔK_{eff} region.

$$\frac{da}{dN} = C_{\text{cg}} \Delta K_{\text{eff}}^{n_{\text{cg}}}, \quad (11)$$

where the constants C_{cg} and n_{cg} have been determined for monolithic aluminium 2024-T3 and have values of respectively $2.17 \cdot 10^{-12}$ and 2.94 for da/dN in [mm/cycle] and ΔK in [MPa/mm].²⁴

EXPERIMENTS

Test specifications

The objective of the experimental program was to obtain detailed knowledge about the crack closure behaviour of FMLs. Therefore, CA fatigue tests have been performed on centre crack tension (CCT) specimens and the crack opening stresses were determined for different stress ratios, similar to the tests performed by Elber on aluminium 2024-T3.⁷ The tests were performed at different maximum stress levels, aluminium sheet thicknesses and GLARE lay-ups. The crack opening stress was also checked at different crack lengths.

The experiments were limited to through-cracks (i.e. cracks with equal length in all metal layers), loaded in the longitudinal direction in a lab air environment at room temperature.

Test matrix

The experiments were performed on GLARE 3 specimens, because this material is currently used in practice and illustrative for other GLARE types, because of its bi-axial fibre orientation.

The first series of experiments was conducted with a GLARE 3-4/3-0.3 'baseline laminate' at various stress ratios between $R = -1$ and $R = 0.6$ to get a direct comparison to the crack opening curve of aluminium 2024-T3.¹⁰ The maximum stress ratio applied was 0.6, because above this level the effective stress range becomes very small. The maximum stress level of these tests was 120 MPa, a level at which reasonable crack growth was achieved.

For the other aluminium thickness (GLARE 3-4/3-0.4) and lay-up (GLARE 3-6/5-0.3), test were performed at three different stress ratios. The 6/5 lay-up is the thickest laminate considered here, because thicker laminates give smaller crack opening as a result of increased fibre restraint. In addition, a possible influence of the maximum stress level was validated with two tests on GLARE 3-4/3-0.3 at 100 and 140 MPa.

The test matrix is given in Table 2. In all experiments, the test specimens were loaded parallel to the rolling direction of the aluminium layers.

Test specimen

The experiments were performed with CCT specimens as illustrated in Fig. 3. Three cracks were used to increase the amount of test data from a single test. The starter

Table 2 Test matrix to determine the crack opening stress level for different stress ratios and laminates

| Material | Maximum stress [MPa] | Stress ratio |
|-----------------|----------------------|--------------|
| GLARE 3-4/3-0.4 | 120 | -0.5 |
| | | 0.02 |
| | | 0.4 |
| GLARE 3-4/3-0.3 | 120 | -1 |
| | | -0.5 |
| | | 0.02 |
| | | 0.1 |
| | | 0.2 |
| | | 0.4 |
| | | 0.6 |
| GLARE 3-6/5-0.3 | 100 | 0.02 |
| | 140 | 0.02 |
| | 120 | -0.5 |
| | | 0.02 |
| | | 0.4 |

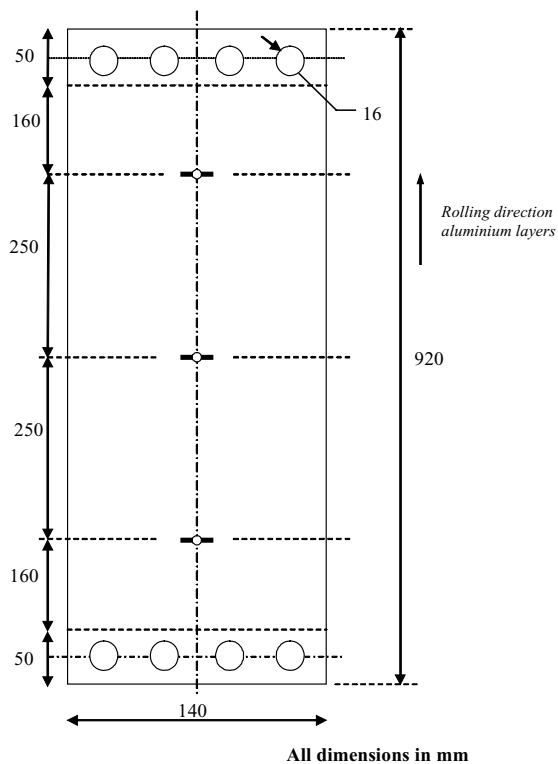


Fig. 3 CCT test specimen configuration.

notches were made by drilling a hole of 2.5 mm diameter with two saw cuts, directing perpendicular to the loading direction. The total length of the starter notch ($2a_0$) was approximately 5 mm. The size of the hole in relation to the final saw-cut length was chosen such, that the presence of the hole has no effect on the stress distribution at the crack tips.

Test equipment

All experiments were performed on the six metric tons MTS[®] fatigue testing machine at the Structures and Materials Laboratory of TUDelft. This machine is closed loop and servo controlled with MTS[®] TestStar[™] (MTS Systems Corporation, Eden Prairie, MN, USA). The load is introduced from the machine mountings into the specimen with bolted clamping. The test frequency was 10 Hz.

For stress ratios below zero, buckling of the specimen was prevented with anti-buckling guides. These guides had to prevent deflection of the test specimen that could cause higher crack growth rates, but were not allowed to carry any load. In addition, the guides were made of non-conducting plywood to enable automatic crack length measurements with the potential drop method (PDM).

Measurement techniques

To determine the crack opening stress, different techniques could be used. In the literature, an extensive

amount of information on this subject can be found.^{7,12,25} In this test program, the crack opening stress was determined with a digital camera. Advantages of a digital camera are the accuracy, the reproducibility and interpretation of results. The image of the digital camera used covers 2.1 by 1.6 mm and with computer software it was possible to record images and measure the crack lengths with an accuracy of 0.01 mm.

The reproducibility and interpretation of the crack image made with the camera for GLARE was better compared to aluminium, because of the limited crack tip plasticity and the limited reflection of the aluminium surface due to the primer.

The observation technique to determine the crack opening with the digital camera was validated with experiments on 2 mm thick aluminium 2024-T3 specimens. The test results of these experiments were identical to the results represented by the curve of Schijve.¹⁰

The crack length was measured with the PDM at the three crack locations on both sides every 5 kcycles. A detailed description of the PDM can be found in the literature.^{26,27} The voltage difference over the crack was normalized with the voltage difference over the total specimen, in accordance with Johnson.²⁶ The calibration curve that related the potential ratio $\Delta v_{\text{crack}}/\Delta v_{\text{specimen}}$ to a crack length consisted of two parts: a second order function for small cracks ($2a < 15$ mm), and a linear part for longer crack lengths ($2a > 15$ mm).

The electrical current (direct current) was lead into the specimen at the bolt connection, by 3-mm thick brass plates. At these locations the specimen was sanded to remove the non-conducting primer. To prevent the current leak through the bolts, Teflon casings were used which covered the bolts.

Discussion of the test results

For each GLARE type the da/dN -a data is presented in Figs. 4–7. In Fig. 4, the test results on GLARE 3-4/3-0.3 loaded under a maximum stress of 120 MPa between stress ratios $R = -1$ and $R = 0.6$ are given. The crack growth curves of the experiments on GLARE 3-4/3-0.4 laminates are given in Fig. 5. In a similar way, the experiments on GLARE 3-6/5-0.3 laminates are presented in Fig. 6.

In every experiment the crack opening stress was measured at 50, 100, 150 and 200 kcycles. In Table 3 an overview of the crack opening stresses for each experiment is presented. These crack opening stresses are independent of crack length: no relation between crack length and the crack opening stress has been observed in the tests.

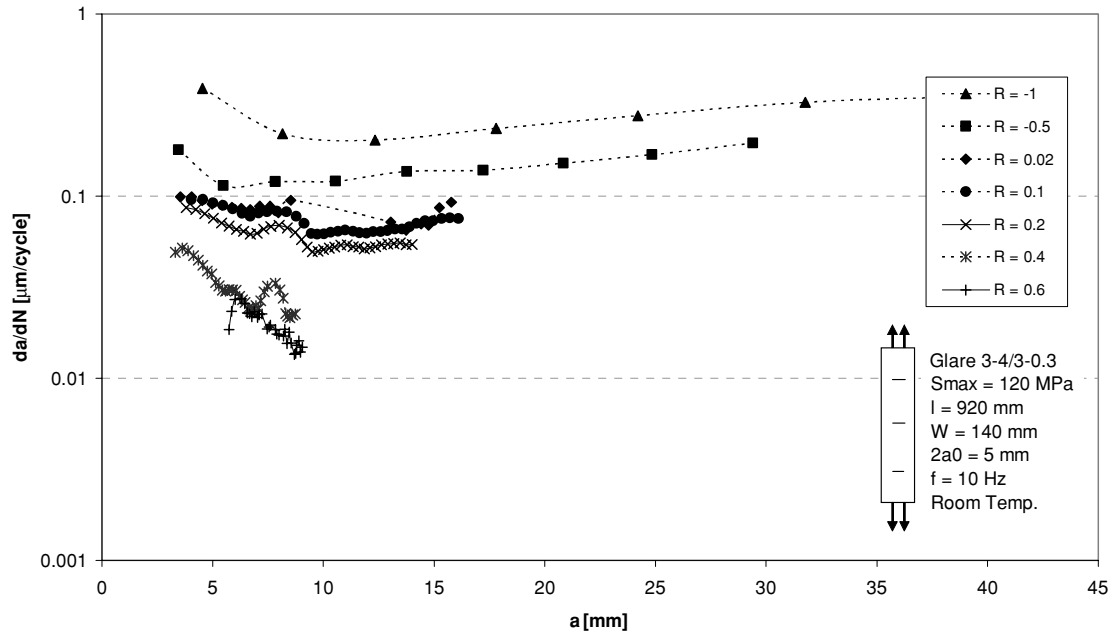


Fig. 4 Crack growth rate versus crack length for GLARE 3-4/3-0.3 loaded with a maximum stress of 120 MPa and under stress ratios of -1 , -0.5 , 0.02 , 0.1 , 0.2 , 0.4 and 0.6 .

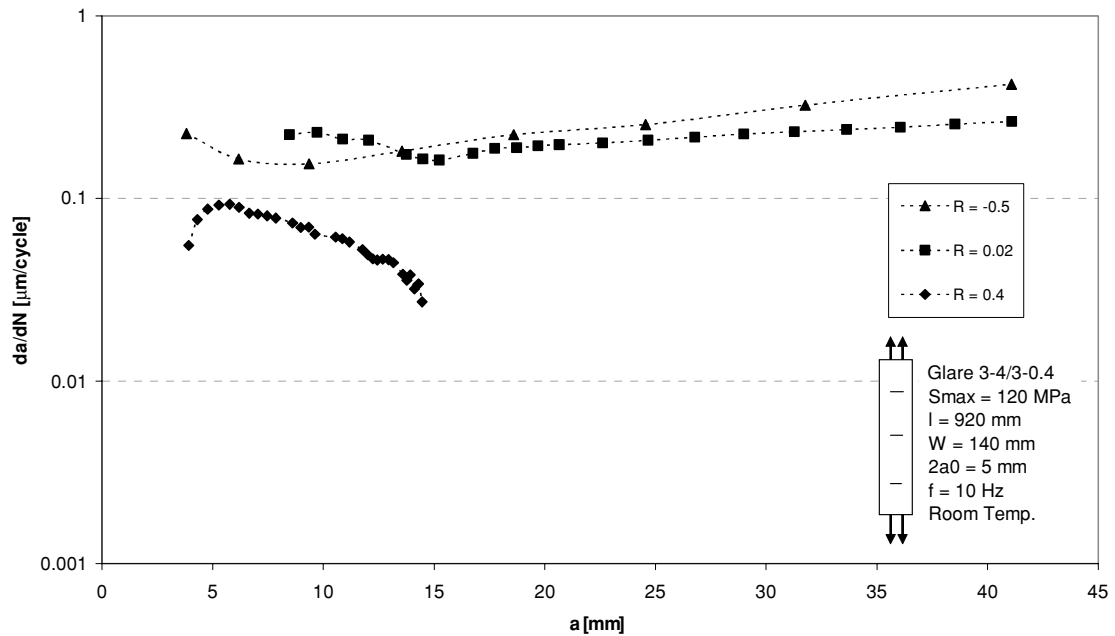


Fig. 5 Crack growth rate versus crack length for GLARE 3-4/3-0.4 loaded with a maximum stress of 120 MPa and under stress ratios of -0.5 , 0.02 and 0.4 .

ANALYSIS AND DISCUSSION OF THE TEST RESULTS

From the test results presented in Table 3, the crack opening ratio (S_{op}/S_{max}) as a function of the applied stress ratio has been determined. A comparison of this ratio for monolithic aluminium¹⁰ and GLARE is presented in Fig. 7. Based on the earlier explained dif-

ferent stress states for different sheet thickness,¹² it could be expected that thin aluminium sheets used in GLARE, have a higher crack opening stress. From this figure it can be seen that the different laminates have different crack opening stresses for equal stress ratios.

The metal volume in the GLARE laminate can be calculated as percentage of the total volume, called the metal

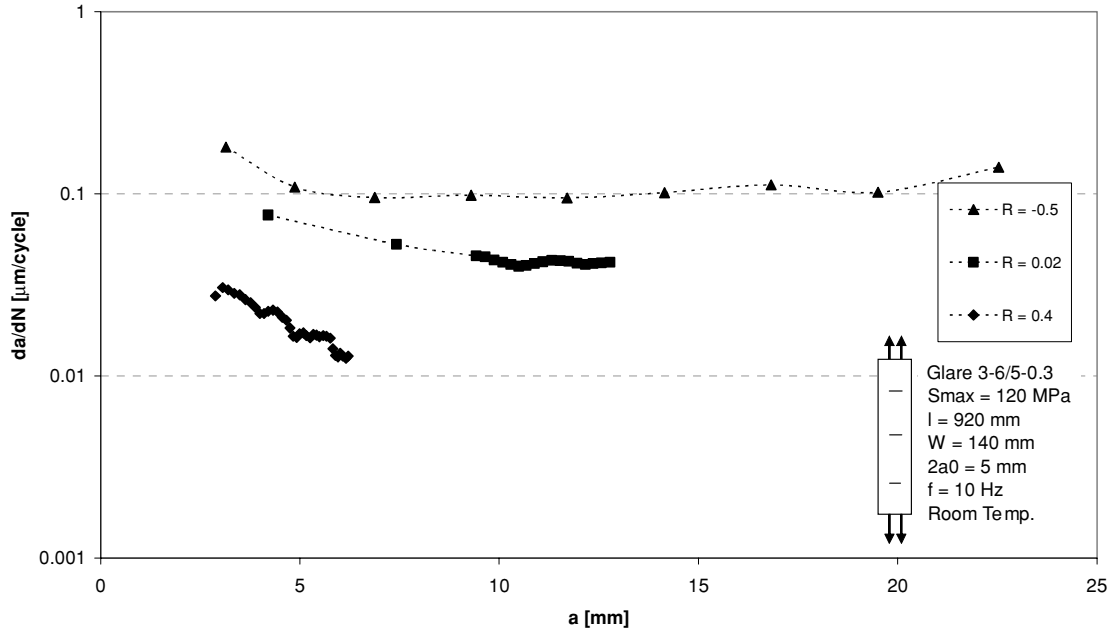


Fig. 6 Crack growth rate versus crack length for GLARE 3-6/5-0.3 loaded with a maximum stress of 120 MPa under stress ratios of -0.5 , 0.02 and 0.4 .

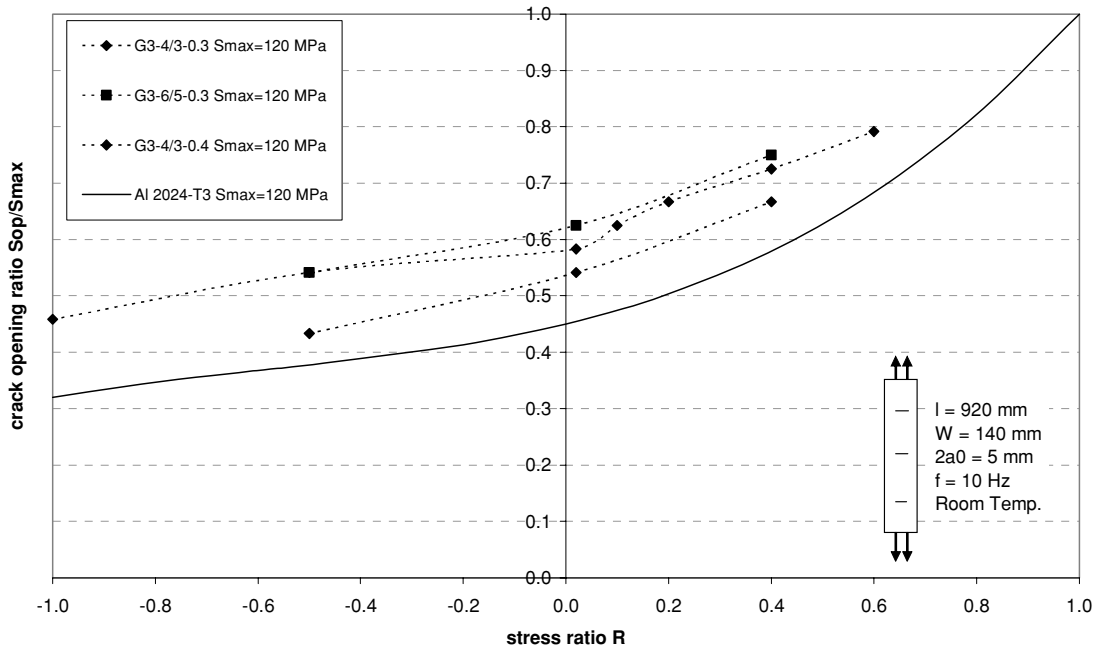


Fig. 7 Crack opening ratio versus stress ratio for different GLARE laminates and maximum stresses loaded with CA fatigue cycles together with the Schijve correction for monolithic aluminium 2024-T3.¹⁰

volume fraction (MVF).^{28,29}

$$MVF = \frac{\sum_{i=1}^{n=i} t_{al}}{t_{lam}} \quad (12)$$

Table 4 presents the calculated MVF for the three laminates. When the test results in Fig. 7 are related to the MVE, it can be concluded that a laminate with a

higher MVF has a lower crack opening ratio. In other words, laminates with a higher MVF behave more like monolithic aluminium, which has according to the definition a MVF of 1.

The stress levels and the stress ratios discussed with the trend shown in Fig. 7 are all laminate stresses. Following from the assumption that similar stress state in the

aluminium layers compared to monolithic aluminium result in similar crack growth behaviour, the stresses should be recalculated to actual stress levels occurring in aluminium layers. The stress level in the aluminium layer is different from the applied stress on the laminate as result

Table 3 Crack opening stresses for all tests

| Test specimen | S_{\max} [MPa] | Stress ratio | S_{op} [MPa] |
|-----------------|------------------|--------------|-----------------------|
| GLARE 3-4/3-0.4 | 120 | -0.5 | 52 |
| | | 0.02 | 65 |
| | | 0.4 | 80 |
| GLARE 3-4/3-0.3 | 120 | -1 | 55 |
| | | -0.5 | 65 |
| | | 0.02 | 70 |
| | | 0.1 | 75 |
| | | 0.2 | 80 |
| | | 0.4 | 85 |
| | | 0.6 | 95 |
| GLARE 3-6/5-0.3 | 120 | -0.5 | 65 |
| | | 0.02 | 75 |
| | | 0.4 | 90 |

Table 4 Metal volume fraction for the tested GLARE laminates

| Material | MVF |
|-----------------|-------|
| GLARE 3-6/5-0.3 | 0.586 |
| GLARE 3-4/3-0.3 | 0.611 |
| GLARE 3-4/3-0.4 | 0.677 |

of the earlier mentioned stiffness and thermal expansion differences of the constituents.

The assumption that the crack closure behaviour of GLARE is based on aluminium can be verified with the following calculation. The SIF in monolithic aluminium can be related to the applied stress level and the crack length with Eq. (8). This relation is not straightforward for Glare as follows from the discussion of the model.^{4,5} However, based on the similarity assumption, one can assume that the SIF for the opening stress level in monolithic aluminium should be identical to the SIF in GLARE at the time the crack opens. This approach is illustrated in Fig. 9, where the relation between the SIF and the stress level is given for monolithic aluminium and GLARE. The relation for GLARE is determined with the analytical model, taking into account the fibre bridging.

In Table 5, the maximum stress level, the stress ratio and the crack opening stress that is calculated with the above-described method is given together with the stress ratio in the aluminium layers of the laminate.

Similar to Fig. 7, the relation between S_{op}/S_{\max} and the stress ratio in the aluminium layers R_{al} is illustrated in Fig. 9.

With Fig. 9, it can be concluded that the crack closure behaviour of GLARE can be based on the crack closure behaviour of aluminium 2024-T3 if the behaviour of GLARE is related to the stresses in the aluminium layers of the laminate.

Despite the deep plane stress state for thin 0.3 mm aluminium sheets, Fig. 9 shows that the correlation with the

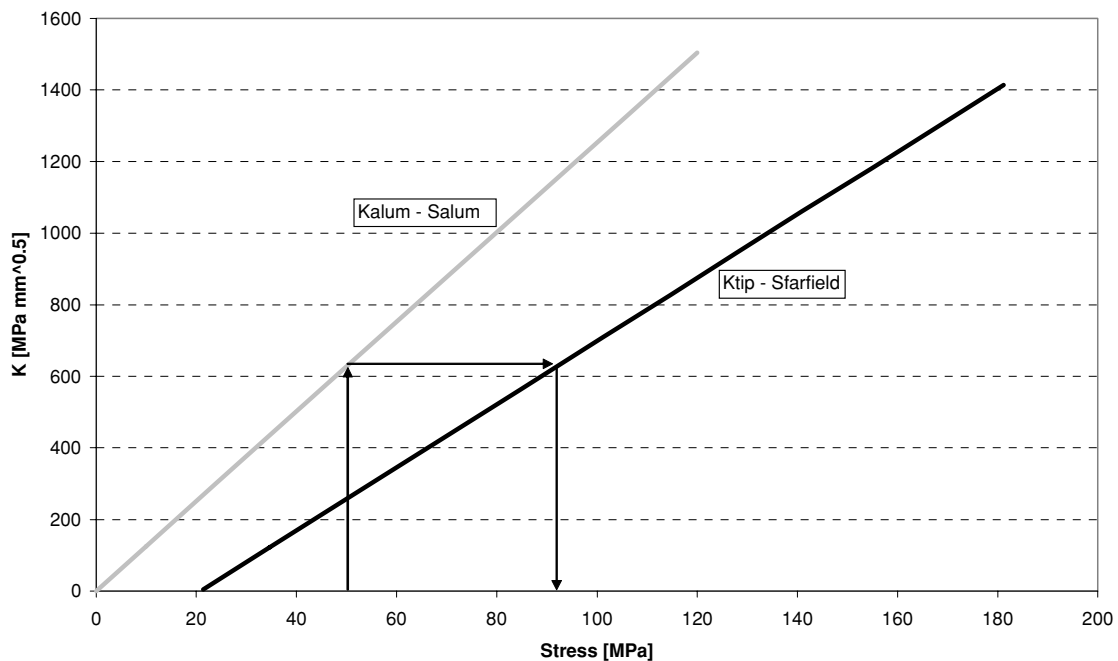


Fig. 8 The far-field stress calculated on the assumption that the stress intensity at the crack tip during crack opening must be similar for both aluminium and GLARE.

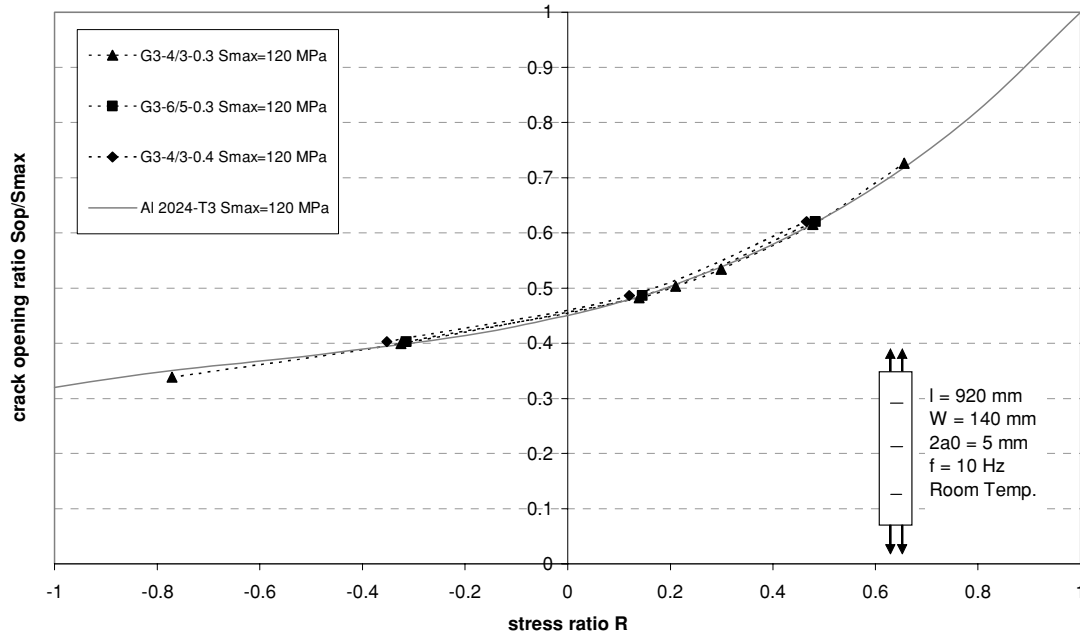


Fig. 9 Crack opening ratio versus stress ratio for different GLARE laminates after recalculation together with the Schijve correction for monolithic aluminium 2024-T3.

Table 5 The maximum stress, stress ratio, and crack opening stress and the stress ratio in the aluminium layers of different GLARE laminates

| Material | GLARE laminate S_{max} (MPa) | GLARE laminate stress ratio | GLARE laminate S_{op} (MPa) | Aluminium stress ratio |
|-----------------|--------------------------------|-----------------------------|-------------------------------|------------------------|
| GLARE 3-4/3-0.4 | 120 | -0.5 | 47 | -0.35 |
| | | 0.02 | 57 | 0.12 |
| | | 0.4 | 73 | 0.47 |
| GLARE 3-4/3-0.3 | 120 | -1 | 41 | -0.77 |
| | | -0.5 | 48 | -0.32 |
| | | 0.02 | 58 | 0.14 |
| | | 0.1 | 60 | 0.21 |
| | | 0.2 | 64 | 0.30 |
| | | 0.4 | 74 | 0.48 |
| GLARE 3-6/5-0.3 | 120 | 0.6 | 87 | 0.66 |
| | | -0.5 | 48 | -0.31 |
| | | 0.02 | 58 | 0.15 |
| | | 0.4 | 74 | 0.48 |

reference curve determined with thicker aluminium is excellent. Apparently, the effect of thin sheet stress state can be neglected in this case, which has also been proven by Homan.³

The negligible differences in the crack opening ratios for different laminates and the curve of monolithic aluminium can be explained by the accuracy of the measurement technique and the ability to observe crack opening for different laminates. For laminates with higher MVF crack opening is easier to detect.

Based on this conclusion, the Alderliesten crack growth model for GLARE is adjusted to incorporate crack clo-

sure. Originally, the Alderliesten model used the empirical relation derived by De Koning (Eq. 10) to calculate the effective stress intensity range in the laminate. With the effective stress intensity range, the crack growth rate can be calculated for the Paris-region with the constants C_{cg} and n_{cg} .

As the constants C_{cg} and n_{cg} have been determined for De Koning correction, they have to be recalculated for the Schijve correction (Eq. 2) to account for the differences in effective stress range:

$$C_{cg} (\Delta K_{eff}^{n_{cg}})_{deKoning} = C_2 (\Delta K_{eff}^{n_2})_{Schijve} \tag{13}$$

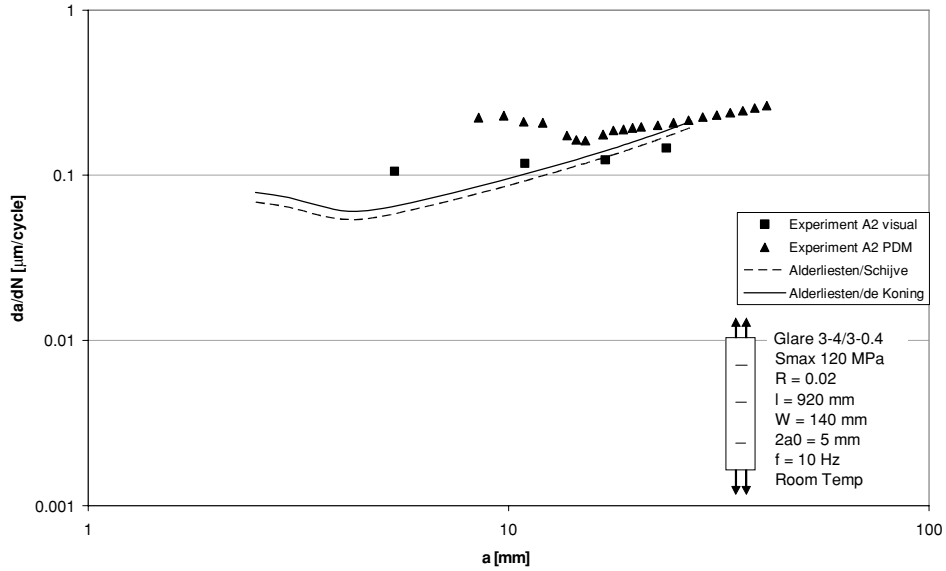


Fig. 10 GLARE 3-4/3-0.4 laminate loaded with S_{max} 120 MPa and $R = 0.02$.

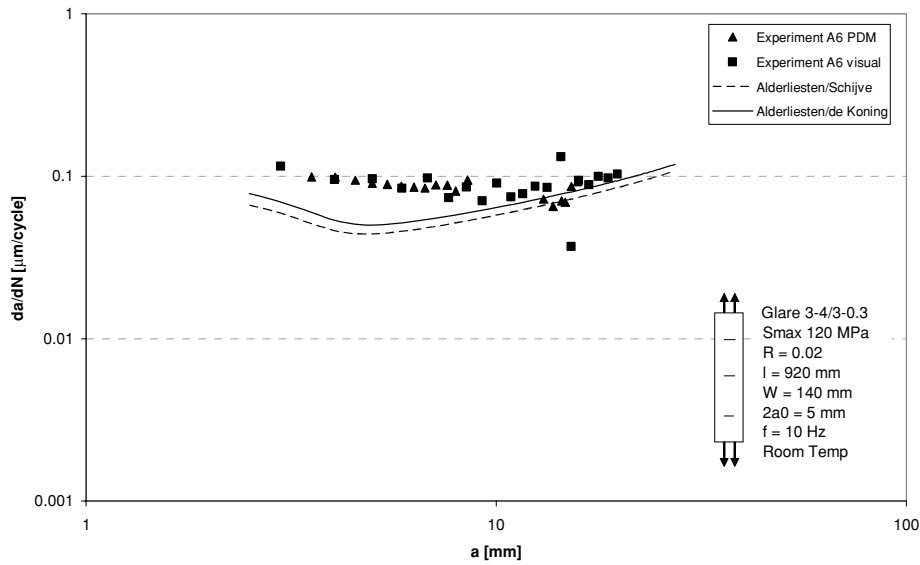


Fig. 11 GLARE 3-4/3-0.3 laminate loaded with S_{max} 120 MPa and $R = 0.02$

where $(\Delta K_{eff})_{deKoning}$ is defined in Eq. (10) and $(\Delta K_{eff})_{Schijve}$ in Eq. (3).

If it is assumed that $n_{cg} = n_2$, the constant C_2 can be calculated and is $1.27 \cdot 10^{-11}$ for ΔK in MPa/mm and da/dN in mm/cycle.

The correction of De Koning and its Paris region constants can now be replaced by the Schijve correction for crack closure and the new constants. The stress ratio in the Schijve correction uses the stress ratio in the aluminium layers to obtain ΔK_{eff} .

$$\Delta K_{eff} = (0.55 + 0.33R_{al} + 0.12R_{al}^2) \Delta K_{tip}. \quad (14)$$

The crack growth can be calculated for the Paris-region with the constants C_2 and n_2 :

$$\left(\frac{da}{dN}\right) = C_2 (\Delta K_{eff})^{n_2}. \quad (15)$$

VALIDATION OF MODEL INCLUDING CRACK CLOSURE CORRECTION

The Alderliesten model with the crack closure correction was validated with test results and with predictions of the Alderliesten model including the empirical relation of

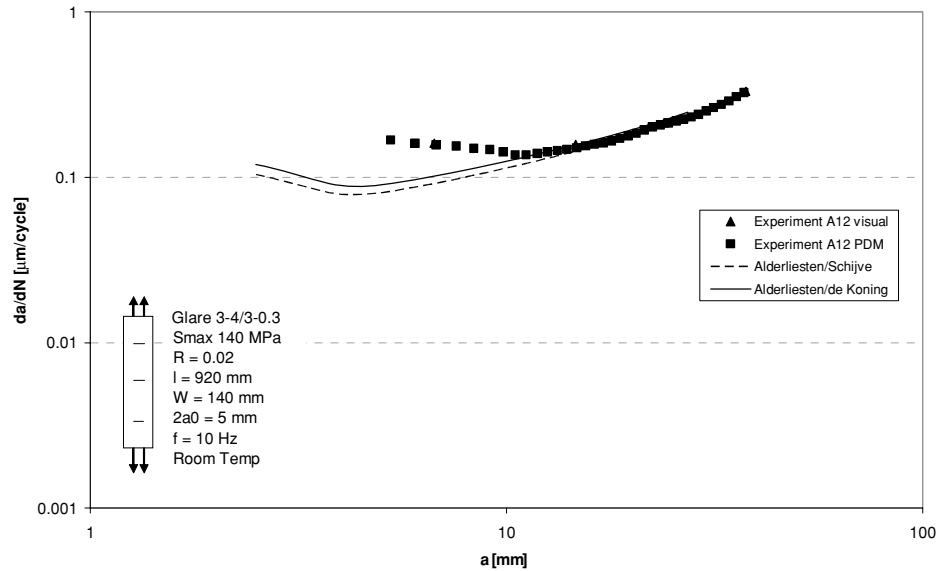


Fig. 12 GLARE 3-4/3-0.3 laminate loaded with S_{max} 140 MPa and $R = 0.02$.

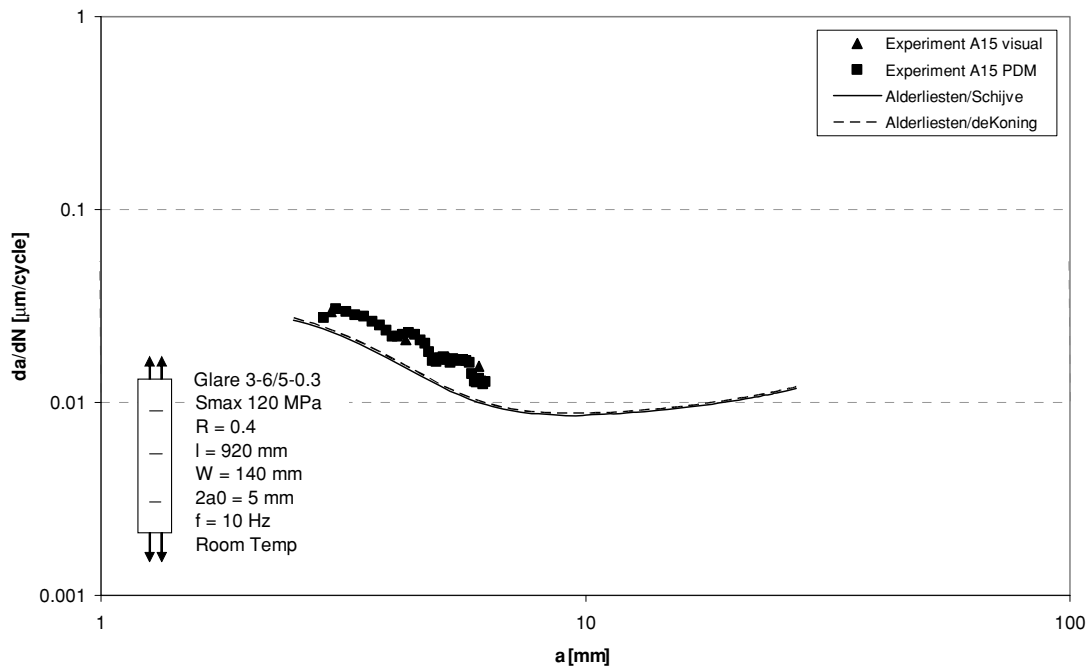


Fig. 13 GLARE 3-6/5-0.3 laminate loaded with S_{max} 120 MPa and $R = 0.4$.

De Koning. The Figs. 10–13 give an illustration of these validations.

The validation of the crack closure correction with both the test results and the predictions of the Alderliesten model including the empirical model of De Koning show a good correlation in crack growth rates. In the Figs. 10–13, the predictions with both corrections coincide. Only for negative stress ratios, not shown here, the crack growth rate is underestimated. This holds for both the crack clo-

sure correction of Schijve and the correction of De Koning and is caused by the Alderliesten model itself. The Alderliesten model has been derived only for positive stress ratios and has not been extended and validated for negative stress ratios.^{4,5}

The crack closure correction can be used for different GLARE lay-ups, aluminium sheet thicknesses and for different applied maximum stresses and stress ratios.

CONCLUSIONS

Crack closure in FMLs has been investigated. Fatigue crack growth experiments on GLARE, an FML of Aluminium 2024-T3 and a prepreg with S2-glass, has been performed with measurement of the crack opening stress level.

The crack opening behaviour of FMLs is similar to monolithic aluminium. Analysis showed that crack growth rates in FMLs are dominated by the metal and can be modelled accordingly if specific FML mechanisms, like fibre bridging, are taken into account.

REFERENCES

- Vlot, A. (2001) *GLARE; history of the development of a new aircraft material*, Kluwer Academic Publishers, Dordrecht, The Netherlands.
- Vlot, A., Gunnink, J. W. (2001) *Fibre Metal Laminates, An Introduction*, Kluwer Academic Publishers, Dordrecht, The Netherlands.
- Homan, J. J. (2006) Fatigue initiation in fibre metal laminates, *Int. J. Fatigue* **28**, 366–374.
- Alderliesten R. C. (2005) *Fatigue Crack Propagation and Delamination Growth in Glare*, PhD. Thesis, Delft University of Technology, Delft.
- Alderliesten R. C. (2007) Analytical prediction model for fatigue crack propagation and delamination growth in Glare, *Int. J. Fatigue* **29**, 628–646.
- Irwin, G. R. (2007) Analysis of stresses and strains near the end of a crack traversing a plate, *Trans. ASME, J. App. Mech.* **24**, 361–364.
- Elber, W. (1971) *The Significance of Fatigue Crack Closure, Damage Tolerance in Aircraft Structures*, ASTM STP 486, pp. 230–242.
- Koning, A. U. de (2001) *Analysis of Fatigue Crack Growth Behaviour of "Through the Thickness" Cracks in Fibre Metal Laminates (FML's)*, Report NLR-CR-2000-575, National Aerospace Laboratory (NLR).
- Newman, J. C. Jr. (1976) *A finite-element analysis of fatigue crack closure, Mechanics of crack growth*, ASTM STP 590, pp. 281–301.
- Schijve, J. (1980) *Some Formulas for the Crack Opening Stress Level, Memorandum M-368*, Delft University of Technology, Delft.
- Shih, T. T., Wei, R. P. (1973) *A study of crack closure in fatigue*, NASA CR 2319.
- Schijve, J. (2001) *Fatigue of Structures and Materials*, Kluwer Academic Publishers, Dordrecht, The Netherlands.
- Schijve, J. (1979) *The Stress Ratio Effect on Fatigue Crack Growth in 2024-T3 Alclad and the Relation to Crack Closure, Memorandum M-336*, Delft University of Technology, Delft.
- Brown, R. D., Weertman, J. (1978) Effect of tensile overloads on crack closure and crack propagation rates in 7050 aluminium, *Eng. Fracture Mech.* **10**, 867–878.
- Trebules, V. W., Roberts, R. Jr., Hertzberg, R. W. (1973) *Effect of multiple overloads on fatigue crack propagation in 2024-T3 aluminium alloy*, ASTM STP 536, pp.115–146.
- Arkema, W. J. (1976) quoted in J. Schijve, *Observations on the prediction of fatigue crack growth under variable-amplitude loading*, ASTM STP 595, pp. 3–23.
- Gan, D., Weertman, J. (1983) Fatigue crack closure after overload, *Eng. Fracture Mech.* **18**, 155–160.
- Blazewicz, W. (1979) Reported by Schijve, J., Lecture II – Fatigue Cracks, Plasticity Effects and Crack Closure, *Eng. Fracture Mech.* **11**, 182–196.
- Suresh, S., Ritchie, R. O. (1982) A geometric model for fatigue crack closure induced fracture surface roughness, *Metallurgical Trans. A.* **13a**, 1627–1631.
- Gray, III, G. T., Williams, J. C., Thompson, A. W. (1983) Roughness induced crack closure: an explanation for microstructurally sensitive fatigue crack growth, *Metallurgical Trans. A.* **14a**, 421–433.
- Suresh, S., Zamaski, G. F., Ritchie, R. O. (1981) Oxide induced crack closure: An explanation for near-threshold corrosion fatigue crack growth behaviour, *Metallurgical Trans. A.* **12a**, 1435–1443.
- Alderliesten, R. C., J.Schijve, and S. van der Zwaag (2006) Application of the energy release rate approach for delamination growth in Glare, *Eng. Fracture Mech.* **73**, 697–709.
- Ewalds, H. L., Wanhill, R. J. H. (1989) *Fracture Mechanics*, Delft University Press, Delft, The Netherlands.
- Homan, J. J. (2002) *Crack growth properties of thin aluminium sheets, Issue 2, Report B2V- 01-16 (Restricted)*, Delft University of Technology, Delft.
- ASTM E 647 (1995) Standard test method for measurements of fatigue crack growth rates. In: *Annual Book of ASTM Standards: Vol. 0301*. Philadelphia: American Society for Testing and Materials, pp. 562–598.
- Johnson, H. H. (1965) *Calibrating the electrical potential method for studying slow crack growth*, Material Research and Standards **5**, pp. 442–445.
- Burgers, A., Kempen, P. D. (1980) *Automatic Crack Length Measurements by the Electrical Potential Drop Method with Computer Control*, Report LR-309, Delft University of Technology, Delft.
- Roebroeks, G. H. J. J. (2000) *The Feasibility of the Metal Volume Fraction Approach for the Calculation of the GLARE Blunt Notch Strength*, Report TD-R-99-005, Structure Laminate Institute, Delft.
- Roebroeks, G. H. J. J. (2000) *The Metal Volume Approach*, Report TD-R-00-003, Structure Laminate Institute, Delft.